

Tunable Weyl Semimetals in Periodically Driven Nodal Line Semimetals

Zhongbo Yan^{1,*} and Zhong Wang^{1,2,†}

¹ *Institute for Advanced Study, Tsinghua University, Beijing, China, 100084*

² *Collaborative Innovation Center of Quantum Matter, Beijing 100871, China*

(Dated: March 17, 2019)

Weyl semimetals and nodal line semimetals are characterized by linear band-touching at nodal points and lines, respectively. We predict that a circularly polarized light drives nodal line semimetals into Weyl semimetals. The Weyl points of the Floquet Weyl semimetal thus obtained are tunable by the incident light, which enables investigations of them in a highly controllable manner. The transition from nodal line semimetals to Weyl semimetals is accompanied by the emergence of a large and tunable anomalous Hall conductivity. Our predictions are experimentally testable in thin films of topological semimetals by either pump-probe ARPES or transport measurement.

PACS numbers: 73.43.-f,71.70.Ej,75.70.Tj

In topology we are concerned with properties invariant under smooth deformations. Remarkable progresses in the last several decades have revealed that topology also underlies many fascinating phenomena in condensed matter physics. After in-depth investigations of topological insulators[1–3], considerable attentions are now focused on topological semimetals. Unlike topological insulators, whose gapless excitations always live at sample boundary, topological semimetals host gapless fermions in the bulk. The two major classes of topological semimetals under intense study are (i) nodal point semimetals and (ii) nodal line semimetals (NLSM). The nodal point semimetals include Dirac semimetals(DSM)[4–14] and Weyl semimetals(WSM)[15–31]. The main feature of the band structures of DSMs and WSMs are the linear band-touching points (“Dirac points” and “Weyl points”), which are responsible for most of their interesting properties, including novel phenomena induced by the chiral anomaly[32–44]. NLSMs[45–61] differ in that they contain band-touching *lines* or *rings*[93], away from which the dispersion is linear.

In this paper we show that periodically driving NLSMs by a circularly polarized light (CPL) creates WSMs, namely, nodal lines become nodal points under light illumination. Our work was motivated by the recent progresses in Floquet topological states [62–73], in particular, Ref.[74] showed that incident light can shift the locations of Weyl points in WSMs. The effect we shall predict in NLSMs is much more dramatic: band-touching lines are replaced by points, thus the dimension of the band-touching manifold is changed. Meanwhile, a large anomalous Hall conductivity tunable by the incident light emerges. Unlike the photoinduced Hall effect in Ref.[74], which is proportional to intensity of incident light, the Hall conductivity in our systems is quite insensitive to the light intensity at low temperature, though it depends sensitively on the incident angle of light. The Fermi arcs of the Floquet WSMs have a simple interpretation, namely, it comes from tilting the drumhead surface dispersion of NLSMs.

The Floquet WSMs derived from NLSMs are highly tunable, in particular, the Weyl points can be freely tuned to any locations on the nodal line. Hopefully this tunability will mo-

tivate further investigations of fascinating properties of topological materials.

Recently, there have appeared experimental evidences of nodal lines in PbTaSe₂[55], ZrSiS[75], ZrSiTe[76], and PtSn₄[77], and quite a few theoretical proposals in Cu₃PdN[53, 54] Ca₃P₂[56] Hg₃As₂[78], and 3D graphene networks[52]. Thus our prediction can be experimentally tested in the near future.

Drive nodal line semimetals to Weyl semimetals.— NLSMs with negligible spin-orbit coupling can be regarded as two copies of spinless systems, thus we shall first consider spinless models for notational simplicity. Near the nodal line, the physics can be captured by two-band models[53, 54, 59]. Our starting point is the model Hamiltonian $\hat{H} = \sum_{\mathbf{k}} \hat{\Psi}_{\mathbf{k}}^{\dagger} \mathcal{H}(\mathbf{k}) \hat{\Psi}_{\mathbf{k}}$ with $\hat{\Psi}_{\mathbf{k}} = (\hat{c}_{\mathbf{k},a}, \hat{c}_{\mathbf{k},b})^T$ and $(\hbar = c = k_B = 1)$

$$\mathcal{H}(\mathbf{k}) = [m - Bk^2]\tau_x + vk_z\tau_z + \epsilon_0(\mathbf{k})\mathbb{I}, \quad (1)$$

where a, b refer to the two orbitals involved, m, B are positive constants with the dimension of energy and inverse-energy, respectively; v refers to the Fermi velocity along z direction; $k^2 = k_x^2 + k_y^2 + k_z^2$, and $\tau_{x,y,z}$ are Pauli matrices acting in orbital space. Although quite simple, this two-band model well describes several candidates of NLSMs[53, 54] in which the spin-orbit coupling can be neglected. The form of $\epsilon_0(\mathbf{k})$ is not crucial and shall be specified later. When $\epsilon_0 = 0$, the energy spectra of this Hamiltonian read

$$E_{\pm, \mathbf{k}} = \pm \sqrt{[m - Bk^2]^2 + v^2 k_z^2}. \quad (2)$$

The nodal ring, on which the two bands touch, is located at the $k_z = 0$ plane and determined by the equation $k_x^2 + k_y^2 = m/B$. The nodal ring is protected by a mirror symmetry, $\mathcal{M}\mathcal{H}(k_x, y, k_z)\mathcal{M}^{-1} = \mathcal{H}(k_x, y, -k_z)$, with $\mathcal{M} = i\tau_x$ [94].

We shall study the effect of a periodic driving on the nodal line semimetal. For the sake of concreteness, suppose that a light beam propagates in the x direction (parallel to the plane of nodal line), with the vector potential

$$\mathbf{A}(t) = A_0(0, \cos(\omega t), \sin(\omega t + \phi)). \quad (3)$$

The choice $\phi = 0$ and $\phi = \pi$ corresponds to right-handed and left-handed circularly polarized light (CPL), respectively. The electromagnetic coupling is given by the Peierls substitution, $\mathcal{H}(\mathbf{k}) \rightarrow \mathcal{H}(\mathbf{k} + e\mathbf{A}(t))$. The full Hamiltonian is time-periodic, thus it can be expanded as $\mathcal{H}(t, \mathbf{k}) = \sum_n \mathcal{H}_n(\mathbf{k})e^{in\omega t}$ with

$$\begin{aligned}\mathcal{H}_0(\mathbf{k}) &= [m - Be^2A_0^2 - Bk^2]\tau_x + vk_z\tau_z, \\ \mathcal{H}_{\pm 1}(\mathbf{k}) &= -eA_0(2B(k_y \mp ie^{\pm i\phi}k_z)\tau_x \pm ie^{\pm i\phi}v\tau_z)/2, \\ \mathcal{H}_{\pm 2}(\mathbf{k}) &= -Be^2A_0^2(1 - e^{\pm i2\phi})\tau_x/4.\end{aligned}\quad (4)$$

and $\mathcal{H}_n = 0$ for $|n| > 2$. In the limit where the driving frequency ω is large compared to the other characteristic energy scales, a reasonable description of the system is in terms of the effective time-independent Hamiltonian[63, 79–82], which is given by

$$\begin{aligned}\mathcal{H}_{\text{eff}}(\mathbf{k}) &= \mathcal{H}_0 + \sum_{n \geq 1} \frac{[\mathcal{H}_{+n}, \mathcal{H}_{-n}]}{n\omega} + \mathcal{O}\left(\frac{1}{\omega^2}\right) \\ &= [\tilde{m} - Bk^2]\tau_x + vk_z\tau_z + \lambda k_y\tau_y + \dots,\end{aligned}\quad (5)$$

where $\lambda = -2e^2BvA_0^2 \cos \phi/\omega$ and $\tilde{m} = m - Be^2A_0^2$. The main effect of the light beam manifests in the $\lambda k_y\tau_y$ term. The energy spectra of \mathcal{H}_{eff} is given by

$$\tilde{E}_{\pm, \mathbf{k}} = \pm \sqrt{[\tilde{m} - Bk^2]^2 + v^2k_z^2 + (\lambda k_y)^2}.\quad (6)$$

Once $\lambda \neq 0$, the energy spectra immediately become gapped except at the two Weyl points $\mathbf{K}_{\pm} = \pm(\sqrt{\tilde{m}/B}, 0, 0)$. We can expand \mathcal{H}_{eff} around the Weyl points as $\mathcal{H}_{\pm}(\mathbf{q}) = \sum_{ij} v_{ij}q_i\tau_j$ with $\mathbf{q} = \mathbf{k} - \mathbf{K}_{\pm}$ referring to the momentum relative to the gapless points, with $v_{xx} = \mp 2\sqrt{\tilde{m}B}$, $v_{yy} = \lambda$, $v_{zz} = v$, and all other matrix entries are zero. The chirality of the Weyl points at \mathbf{K}_{\pm} is $\chi_{\pm} \equiv \text{sgn}[\det(v_{ij})] = \pm \text{sgn}(\cos \phi)$. The appearance of $\cos \phi$ implies that the chirality, which is the topological charge of the Weyl points, has a simple dependence on the handedness of the incident laser beam, thus reversing the handedness causes the reversing of the chirality of Weyl points. Moreover, the locations of the Weyl points is tunable by changing the direction of the incident laser beams. For instance, the two Weyl points would be located at $\pm(0, \sqrt{\tilde{m}/B}, 0)$ if the laser beam is along the y direction.

If one considers a nodal ring of generic shape and the incident light along x direction, one can show that Weyl points are created around the local maxima and local minima of k_x on the nodal ring, and the chirality of the Weyl point is opposite on the maxima and minima. It is readily seen that the number of local minima and that of local maxima are equal on a ring[95], therefore, the Nielsen-Ninomiya theorem[83], which states that the equality of the numbers of Weyl points with opposite chirality, is automatically satisfied.

Anomalous Hall effect (AHE).— One of the significant consequences of the topological transition from NLSM to WSM is the emergence of AHE characterized by a non-zero Hall conductivity. The conductivity can be obtained from the linear response theory[64], which leads to

$$\sigma_{\mu\nu} = e^2\epsilon_{\mu\nu\rho} \int \frac{d^3k}{(2\pi)^3} \sum_{\alpha} f_{\alpha}(k)[\nabla_{\mathbf{k}} \times \mathcal{A}_{\alpha}(\mathbf{k})]_{\rho}\quad (7)$$

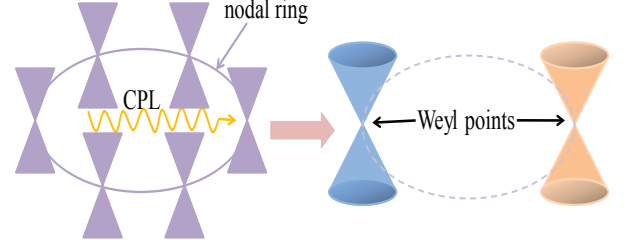


FIG. 1: Conceptual view for the emergence of Weyl points from nodal line semimetal. A nodal line (or nodal ring) semimetal can be regarded as infinite copies of two-dimensional Dirac semimetal, with linear dispersion in the two directions perpendicular to the nodal ring. An incident circularly polarized light(CPL) leaves only two isolated points gapless, near which the dispersion is linear in all three directions, as described by the Weyl equation. The different colors of the Weyl cones represent different chirality (± 1).

where $\mu, \nu, \rho = x, y, z$ and $\epsilon_{\mu\nu\rho} = \pm 1$ for even (odd) permutation of (x, y, z) , $\alpha \equiv (i, n)$, with i referring to the original band index and n referring to the Floquet index, $\mathcal{A}_{\alpha}(\mathbf{k})$ is the Berry connection[64], and f_{α} is the occupation function. Thus the Hall conductivity depends not only on the Berry curvature but also on the fermion occupation, the later of which is nonuniversal, being dependent on details of the systems (e.g. the coupling between the systems and the bath). Below we shall focus on the case that the occupation is close to equilibrium, namely, $f_{(i,n)} = \delta_{n0}n_i(E_{i,\mathbf{k}})$, where $n_i(E_{i,\mathbf{k}})$ is the Fermi-Dirac distribution. For the incident light beams along the x direction, the interesting component of the Hall conductivity is σ_{yz} , which can be found as (Supplemental Material)

$$\begin{aligned}\sigma_{yz}(T, \mu) &= \frac{e^2}{2} \int \frac{d^3k}{(2\pi)^3} [\hat{\mathbf{d}} \cdot (\frac{\partial \hat{\mathbf{d}}}{\partial k_y} \times \frac{\partial \hat{\mathbf{d}}}{\partial k_z})](n_+ - n_-) \\ &= \frac{e^2}{2} \int \frac{d^3k}{(2\pi)^3} \frac{\lambda v(\tilde{m} - 2Bk_x^2 + Bk^2)}{\tilde{E}_{+, \mathbf{k}}^3} (n_+ - n_-),\end{aligned}\quad (8)$$

where $\hat{\mathbf{d}} = \mathbf{d}/|\mathbf{d}|$ with $\mathbf{d} = \text{Tr}[\nabla_{\mathbf{k}} \mathcal{H}_{\text{eff}}]/2$, and $n_{\pm} = 1/(e^{(\tilde{E}_{\pm, \mathbf{k}} - \mu)/T} + 1)$ is the Fermi-Dirac distribution with μ denoting the chemical potential. From Eq.(8), it is readily seen that when $\lambda = 0$, σ_{yz} vanishes identically, indicating the absence of AHE in the pristine NLSM. For non-zero temperature ($T \neq 0$) or doped system ($\mu \neq 0$), analytic simplification of Eq.(8) is not available, and we need to treat Eq.(8) numerically. We find that in the small λ regime, $|\sigma_{yz}|$ increases monotonically with λ , however, $|\sigma_{yz}|$ saturates at larger λ , as can be appreciated from Fig.2. The saturation is quicker at lower temperature.

At $T = 0$ and $\mu = 0$, a simple analytic expression follows from Eq.(8):

$$\begin{aligned}\sigma_{yz}(0, 0) &= \frac{e^2}{2\pi} \text{sgn}(\cos \phi) \int_{-\infty}^{+\infty} \frac{dk_x}{2\pi} \Theta(\tilde{m} - Bk_x^2) \\ &= \frac{e^2}{\pi h} \sqrt{\frac{m}{B} - e^2A_0^2} \text{sgn}(\cos \phi),\end{aligned}\quad (9)$$

At the last step, we have restored the Planck constant h . It is readily seen that $\sigma_{yz}(0, 0)$ is proportional to the distance

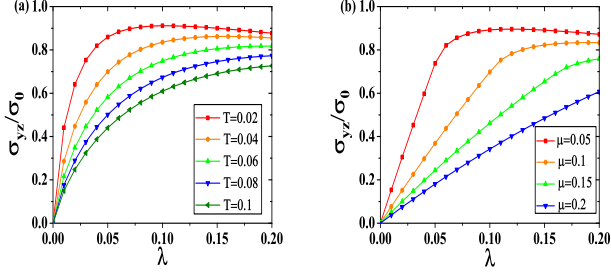


FIG. 2: The dependence of Hall conductivity on temperature (T), chemical potential (μ) and the intensity of the incident light beam λ . The common parameters in use are $m = 1$, $B = 1$, $\omega = 2$, $\phi = \pi$, $v = 1$, $\epsilon_0 = 0$, and we have defined the shorthand notation $\sigma_0 = \frac{e^2}{\pi h} \sqrt{\frac{m}{B}}$. (a) σ_{yz} at $\mu = 0$ as a function of λ for several values of T ; (b) σ_{yz} at $T = 0$ as a function of λ for several values of μ .

between the two Weyl points. The Hall conductivity can be easily tuned by the incident angle of light. For instance, the nonzero component would be σ_{xz} instead of σ_{yz} if the incident light is along the y direction.

This behavior is remarkably different from the light-induced Hall effect in Weyl semimetals (see Ref.[74]), for which the Hall conductivity is proportional to A_0^2 , which becomes weak when $A_0 \rightarrow 0$. The proposal of Ref.[74] is to separate existing Weyl points in WSMs by light, while ours is to create Weyl points from NLSMs. The former is a second-order effect proportional to A_0^2 , while the AHE in the present work is a zeroth-order effect, which should be much more pronounced in experiment. In general, the distance between the two photoinduced Weyl points is of the order of $2\pi/a$, a referring to the lattice constant, thus we have the estimation $\sigma_{yz} \sim (e^2/h)(2\pi/a)$.

Fermi arc as the descendent of drumhead states.— The dispersion of the surface states of the NLSM take the shape of a drumhead or a bowl, i.e., a nearly flat band bounded by the projection of the bulk nodal line to the surface Brillouin zone. When $\epsilon_0 = 0$, the dispersion becomes exactly flat. Since the NLSM is driven to a WSM phase in our study, it is a natural question how the surface state evolves from a drumhead (or bowl) to a Fermi arc. We consider a semi-infinite geometry, namely, the sample occupies the entire $z > 0$ half-space. The \mathbf{k} -space energy eigenvalue problem is translated to the real space as $\mathcal{H}_{\text{eff}}(k_x, k_y, -i\partial_z)\Psi(z) = E(k_x, k_y)\Psi(z)$, under the boundary conditions $\Psi(0) = 0$ and $\Psi(+\infty) = 0$, the later one ensuring the normalizability of the wavefunction.

We find that the surface modes wavefunction takes the form of

$$\Psi(x, y, z) = \mathcal{N} e^{ik_x x} e^{ik_y y} \sin(\kappa z) e^{-\gamma z} \chi, \quad (10)$$

with

$$E(k_x, k_y) = -\lambda k_y + \epsilon_0(k_x, k_y), \quad (11)$$

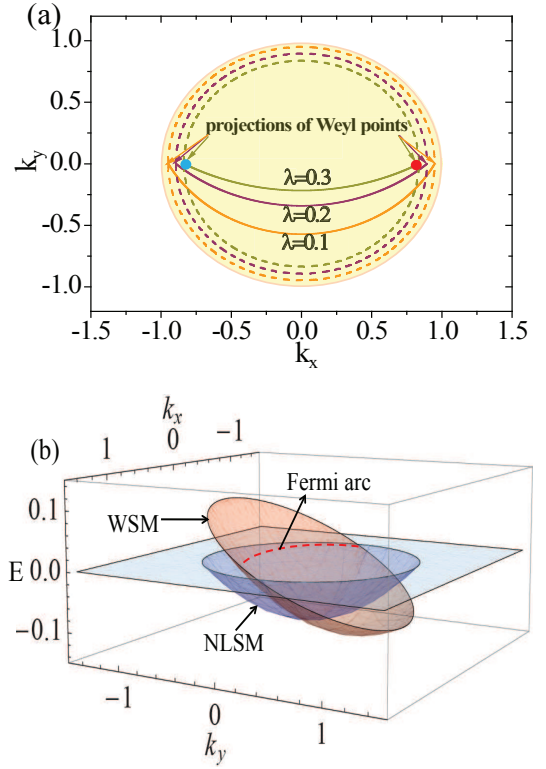


FIG. 3: The surface states dispersions of the NLSM and the Floquet WSM. The values of parameters are taken to be $m = B = 1$, $\omega = 2$, $\phi = \pi$, $v = 1$, and $\epsilon_0(k) = 0.1(k_x^2 + k_y^2)$. The chemical potential has been tuned to the Weyl band-touching points. (a) Top view. The shadow area ($k_x^2 + k_y^2 < m/B$) represents the drumhead surface states of the pristine NLSM without incident light, and the dashed lines enclose the area for which the surface states exist in the Floquet WSM ($k_x^2 + k_y^2 < \tilde{m}/B$), with the three colors referring to three values of λ , as indicated in the figure. The solid curves are the Fermi arcs connecting the projections of the two Weyl points onto the surface Brillouin zone. (b) Side view. The surface state dispersions of both the pristine NLSM and the Floquet WSM (with the driving parameter $\lambda = 0.1$) are shown. Tilting the surface state dispersion of the NLSM leads to that of the WSM. The intersection of the dispersion of WSM and the $E = 0$ plane is the Fermi arc.

where $\chi = (1, -i)^T / \sqrt{2}$, \mathcal{N} is a normalization factor, and

$$\gamma = \frac{v}{2B}, \quad \kappa = \frac{1}{2B} \sqrt{2B[\tilde{m} - B(k_x^2 + k_y^2)] - v^2}. \quad (12)$$

Implicit here is that $2B[\tilde{m} - B(k_x^2 + k_y^2)] - v^2 > 0$, so that κ is real-valued; in the cases of $2B[\tilde{m} - B(k_x^2 + k_y^2)] - v^2 < 0$, the solution can be obtained by replacing $\sin(\kappa z)$ by $\sinh(|\kappa|z)$, namely,

$$\Psi(x, y, z) = \mathcal{N} e^{ik_x x} e^{ik_y y} \sinh(|\kappa|z) e^{-\gamma z} \chi, \quad (13)$$

It can be found that the normalizability requires

$$k_x^2 + k_y^2 < \tilde{m}/B, \quad (14)$$

which determines the region where the surface modes exist. It is notable that the dispersion given by Eq.(11) shows a chiral

nature in the y direction. As a comparison, we note that the surface states of the NLSM can be recovered by letting $\lambda = 0$, which, according to Eq.(11), leads to the dispersion of the drumhead/bowl states: $E(k_x, k_y) = \epsilon_0(k_x, k_y)$. The region of the drumhead/bowl is given by Eq.(14) with \tilde{m} replaced by m , namely, $k_x^2 + k_y^2 < m/B$. An illustration can be found in Fig.(3a), in which the surface state of the pristine NLSM is represented by the shadow area, and the surface states of the Floquet WSM for three values of intensity of incident laser are enclosed by the three dashed lines with different colors. Due to the nonzero λ generated by the incident laser, which enters Eq.(11), the dispersion of the drumhead/bowl states of the pristine NLSM becomes tilted (see Fig.3b).

Spinful systems.— The main results presented above can be generalized to spinful systems with spin-orbit coupling, with the main picture unchanged. For concreteness, we consider a model Hamiltonian $\mathcal{H}_s(\mathbf{k}) = (m - Bk^2)\tau_x + vk_z\tau_z + \Delta_{so}\tau_x s_z$, where s_z is the Pauli matrix associated with the spin degree of freedom, and Δ_{so} quantifies the spin-orbit coupling. This model hosts two nodal lines, and is relevant to the NLSM candidate TlTaSe₂[60]. Using the method of the previous sections, we can find the effective Floquet Hamiltonian $\mathcal{H}_{s,\text{eff}}(\mathbf{k}) = (m - Bk^2)\tau_x + vk_z\tau_z + \Delta_{so}\tau_x s_z + \lambda k_y\tau_y$, with spectrum $E = \pm \sqrt{(\tilde{m} \pm \Delta_{so} - Bk^2)^2 + v^2 k_z^2 + \lambda^2 k_y^2}$, in which the expressions for λ and \tilde{m} are the same as given below Eq.5. Thus the system is driven to the WSM phase with four Weyl points at $\mathbf{K}_1^\pm = \pm(\sqrt{(\tilde{m} + \Delta_{so})/B}, 0, 0)$ and $\mathbf{K}_2^\pm = \pm(\sqrt{(\tilde{m} - \Delta_{so})/B}, 0, 0)$.

Effect of a small gap.— In several candidates of NLSMs, the nodal line can be gapped out if a small spin-orbit coupling[53, 54, 78] is included. Below we shall show that such a small gap mainly introduces a threshold laser intensity for the generation of Weyl points. Let us consider the model

$$\mathcal{H}_g(\mathbf{k}) = (m - Bk^2)\tau_x + vk_z\tau_z + \lambda_{so}\tau_y s_z. \quad (15)$$

where s_z refers to the z component of spin, and the $\lambda_{so}\tau_y s_z$ term induces an energy gap $2|\lambda_{so}|$. With an incident laser, the effective Hamiltonian reads

$$\mathcal{H}_{g,\text{eff}}(\mathbf{k}) = (m - Bk^2)\tau_x + vk_z\tau_z + \lambda_{so}\tau_y s_z + \lambda k_y\tau_y, \quad (16)$$

with spectrum $E = \pm \sqrt{(\tilde{m} - Bk^2)^2 + v^2 k_z^2 + (\lambda k_y \pm \lambda_{so})^2}$. There are clearly four generated Weyl points, located at $\mathbf{Q}_1^\pm = (\pm \sqrt{\tilde{m}/B - (\lambda_{so}/\lambda)^2}, \lambda_{so}/\lambda, 0)$, and $\mathbf{Q}_2^\pm = (\pm \sqrt{\tilde{m}/B - (\lambda_{so}/\lambda)^2}, -\lambda_{so}/\lambda, 0)$. It is readily seen that the main effects of the gap are: (i) There is a threshold laser intensity $\lambda_{\text{th}} = \sqrt{\lambda_{so}^2 B/\tilde{m}}$, above which the Weyl points can be generated; (ii) The locations of the Weyl points are shifted compared to the $\lambda_{so} = 0$ case.

Experimental considerations.— Among other possibilities, it should be feasible to test our predictions in thin film of NLSMs. The incident light has a finite penetration depth ξ , and it would be most efficient to measure the Hall conductivity in film with thickness $\sim \xi$. The estimation of ξ becomes

simple when the Fermi velocities along the z direction and the x - y direction are the same, namely, when $2\sqrt{mB} = v$, and the optical absorption rate can be straightforwardly estimated following Ref.[84], leading to $\xi \sim \sqrt{B/(m\alpha^2)}$, where $\alpha \sim 1/137$ is the fine structure constant. Since $\sqrt{B/m}$ is the inverse of the radius of the nodal ring, we expect that it is of the order of a few lattice constant, thus $\xi \sim$ several hundreds of lattice constant. Thin film of NLSM with this thickness should be most suitable experimentally.

Within current experimental feasibility[85], $2e^2 v^2 A_0^2/\omega \sim 50\text{meV}$ is attainable at photon energy $\hbar\omega = 120\text{meV}$ (see Ref.[85]), therefore, if we take $v^2/B \sim 0.5\text{eV}$, we have $|\lambda| \sim 0.1v$. Since we have shown that the Fermi velocity of Fermi arc is λ , we can see that, within the current experimental feasibility, it can reach a tenth of the bulk Fermi velocity of the NLSMs. This can be detected by the pump-probe ARPES[85].

Conclusions.— In this paper we have predicted that Weyl points can be generated in NLSMs by periodic driving, which can be tested by putting a NLSM in circularly polarized light or by shaking lattice[86–88] in cold atom systems with nodal line. The resultant Floquet WSMs have a large AHE controllable by the laser beams. For instance, reversing the handedness of the incident light changes the sign of the anomalous Hall conductivity. The Fermi arcs of the Floquet WSMs have an appealing interpretation, namely, they come from tilting the drumhead surface state of NLSMs. The photoinduced Fermi arcs and the bulk Weyl points can be detected in the pump-probe ARPES, and the AHE can be measured in transport experiments.

Apart from potential applications of the large and tunable AHE in high-speed electronics, the tunability of the Floquet WSMs will also facilitate the future investigations of many novel physics therein by techniques absent in the static systems (e.g. spatial modulation of light [89]). From a broader perspective, our work suggests that Floquet topological semimetals are fruitful platforms in the study of topological matters.

Acknowledgements. This work is supported by NSFC under Grant No. 11304175.

* yzhbo@mail.tsinghua.edu.cn

† wangzhongemail@tsinghua.edu.cn

- [1] M. Z. Hasan and C. L. Kane, Rev. Mod. Phys. **82**, 3045 (2010).
- [2] X.-L. Qi and S.-C. Zhang, Rev. Mod. Phys. **83**, 1057 (2011).
- [3] C.-K. Chiu, J. C. Y. Teo, A. P. Schnyder, and S. Ryu, ArXiv e-prints (2015), 1505.03535.
- [4] Z. Liu, B. Zhou, Y. Zhang, Z. Wang, H. Weng, D. Prabhakaran, S.-K. Mo, Z. Shen, Z. Fang, X. Dai, et al., Science **343**, 864 (2014).
- [5] M. Neupane, S.-Y. Xu, R. Sankar, N. Alidoust, G. Bian, C. Liu, I. Belopolski, T.-R. Chang, H.-T. Jeng, H. Lin, et al., Nature Communications **5**, 3786 (2014), 1309.7892.
- [6] S. Borisenko, Q. Gibson, D. Evtushinsky, V. Zabolotnyy, B. Büchner, and R. J. Cava,

- Phys. Rev. Lett. **113**, 027603 (2014), URL <http://link.aps.org/doi/10.1103/PhysRevLett.113.027603>
- [7] S.-Y. Xu, C. Liu, S. K. Kushwaha, R. Sankar, J. W. Krizan, I. Belopolski, M. Neupane, G. Bian, N. Alidoust, T.-R. Chang, et al., *Science* **347**, 294 (2015).
- [8] Z. Wang, Y. Sun, X.-Q. Chen, C. Franchini, G. Xu, H. Weng, X. Dai, and Z. Fang, *Physical Review B* **85**, 195320 (2012).
- [9] S. M. Young, S. Zaheer, J. C. Teo, C. L. Kane, E. J. Mele, and A. M. Rappe, *Physical review letters* **108**, 140405 (2012).
- [10] Z. Wang, H. Weng, Q. Wu, X. Dai, and Z. Fang, *Physical Review B* **88**, 125427 (2013).
- [11] A. Sekine and K. Nomura, *Phys. Rev. B* **90**, 075137 (2014), URL <http://link.aps.org/doi/10.1103/PhysRevB.90.075137>.
- [12] C. Zhang, E. Zhang, Y. Liu, Z.-G. Chen, S. Liang, J. Cao, X. Yuan, L. Tang, Q. Li, T. Gu, et al., ArXiv e-prints (2015), 1504.07698.
- [13] R. Y. Chen, Z. G. Chen, X.-Y. Song, J. A. Schneeloch, G. D. Gu, F. Wang, and N. L. Wang, *Phys. Rev. Lett.* **115**, 176404 (2015), URL <http://link.aps.org/doi/10.1103/PhysRevLett.115.176404>.
- [14] X. Yuan, C. Zhang, Y. Liu, C. Song, S. Shen, X. Sui, J. Xu, H. Yu, Z. An, J. Zhao, et al., ArXiv e-prints (2015), 1510.00907.
- [15] X. Wan, A. M. Turner, A. Vishwanath, and S. Y. Savrasov, *Phys. Rev. B* **83**, 205101 (2011).
- [16] H. B. Nielsen and M. Ninomiya, *Physics Letters B* **130**, 389 (1983).
- [17] G. E. Volovik, *The Universe in a Helium Droplet* (Oxford University Press, USA, 2003).
- [18] K.-Y. Yang, Y.-M. Lu, and Y. Ran, *Phys. Rev. B* **84**, 075129 (2011), URL <http://link.aps.org/doi/10.1103/PhysRevB.84.075129>.
- [19] A. A. Burkov and L. Balents, *Phys. Rev. Lett.* **107**, 127205 (2011), URL <http://link.aps.org/doi/10.1103/PhysRevLett.107.127205>.
- [20] H. Weng, C. Fang, Z. Fang, B. A. Bernevig, and X. Dai, *Phys. Rev. X* **5**, 011029 (2015).
- [21] S.-M. Huang, S.-Y. Xu, I. Belopolski, C.-C. Lee, G. Chang, B. Wang, N. Alidoust, G. Bian, M. Neupane, A. Bansil, et al., *Nature Communications* **6**, 7373 (2015).
- [22] C. Zhang, Z. Yuan, S. Xu, Z. Lin, B. Tong, M. Zahid Hasan, J. Wang, C. Zhang, and S. Jia, ArXiv e-prints (2015), 1502.00251.
- [23] S.-Y. Xu, I. Belopolski, N. Alidoust, M. Neupane, C. Zhang, R. Sankar, S.-M. Huang, C.-C. Lee, G. Chang, B. Wang, et al., ArXiv e-prints (2015), 1502.03807.
- [24] B. Q. Lv, H. M. Weng, B. B. Fu, X. P. Wang, H. Miao, J. Ma, P. Richard, X. C. Huang, L. X. Zhao, G. F. Chen, et al., ArXiv e-prints (2015), 1502.04684.
- [25] X. Huang, L. Zhao, Y. Long, P. Wang, D. Chen, Z. Yang, H. Liang, M. Xue, H. Weng, Z. Fang, et al., *Phys. Rev. X* **5**, 031023 (2015), URL <http://link.aps.org/doi/10.1103/PhysRevX.5.031023>.
- [26] L. Yang, Z. Liu, Y. Sun, H. Peng, H. Yang, T. Zhang, B. Zhou, Y. Zhang, Y. Guo, M. Rahn, et al., ArXiv e-prints (2015), 1507.00521.
- [27] N. Ghimire, Y. Luo, M. Neupane, D. Williams, E. Bauer, and F. Ronning, *Journal of Physics: Condensed Matter* **27**, 152201 (2015).
- [28] C. Shekhar, A. K. Nayak, Y. Sun, M. Schmidt, M. Nicklas, I. Leermakers, U. Zeitler, Y. Skourski, J. Wosnitza, Z. Liu, et al., *Nature Physics* **11**, 645 (2015).
- [29] S.-Y. Xu, N. Alidoust, I. Belopolski, C. Zhang, G. Bian, T.-R. Chang, H. Zheng, V. Strokov, D. S. Sanchez, G. Chang, et al., ArXiv e-prints (2015), 1504.01350.
- [30] L. Lu, Z. Wang, D. Ye, L. Ran, L. Fu, J. D. Joannopoulos, and M. Soljačić, *Science* **349**, 622 (2015), URL <http://www.sciencemag.org/content/349/6248/622.abstract>.
- [31] L. Lu, L. Fu, J. D. Joannopoulos, and M. Soljačić, *Nature photonics* **7**, 294 (2013).
- [32] D. T. Son and B. Z. Spivak, ArXiv e-prints (2012), 1206.1627.
- [33] C.-X. Liu, P. Ye, and X.-L. Qi, ArXiv e-prints (2012), 1204.6551.
- [34] V. Aji, *Phys. Rev. B* **85**, 241101 (2012), URL <http://link.aps.org/doi/10.1103/PhysRevB.85.241101>.
- [35] A. A. Zyuzin and A. A. Burkov, ArXiv e-prints (2012), 1206.1868.
- [36] Z. Wang and S.-C. Zhang, *Phys. Rev. B* **87**, 161107 (2013), URL <http://link.aps.org/doi/10.1103/PhysRevB.87.161107>.
- [37] P. Hosur and X.-L. Qi, *Phys. Rev. B* **91**, 081106 (2015), URL <http://link.aps.org/doi/10.1103/PhysRevB.91.081106>.
- [38] P. Hosur and X. Qi, *Comptes Rendus Physique* **14**, 857 (2013), 1309.4464.
- [39] H.-J. Kim, K.-S. Kim, J.-F. Wang, M. Sasaki, N. Satoh, A. Ohnishi, M. Kitaura, M. Yang, and L. Li, *Phys. Rev. Lett.* **111**, 246603 (2013), URL <http://link.aps.org/doi/10.1103/PhysRevLett.111.246603>.
- [40] S. A. Parameswaran, T. Grover, D. A. Abanin, D. A. Pesin, and A. Vishwanath, *Phys. Rev. X* **4**, 031035 (2014), URL <http://link.aps.org/doi/10.1103/PhysRevX.4.031035>.
- [41] J. Zhou, H.-R. Chang, and D. Xiao, *Phys. Rev. B* **91**, 035114 (2015), URL <http://link.aps.org/doi/10.1103/PhysRevB.91.035114>.
- [42] Q. Li, D. E. Kharzeev, C. Zhang, Y. Huang, I. Pletikoscic, A. V. Fedorov, R. D. Zhong, J. A. Schneeloch, G. D. Gu, and T. Valla, ArXiv e-prints (2014), 1412.6543.
- [43] R. Bi and Z. Wang, *Phys. Rev. B* **92**, 241109 (2015), URL <http://link.aps.org/doi/10.1103/PhysRevB.92.241109>.
- [44] P. Goswami, J. H. Pixley, and S. Das Sarma, *Phys. Rev. B* **92**, 075205 (2015), URL <http://link.aps.org/doi/10.1103/PhysRevB.92.075205>.
- [45] A. A. Burkov, M. D. Hook, and L. Balents, *Phys. Rev. B* **84**, 235126 (2011), URL <http://link.aps.org/doi/10.1103/PhysRevB.84.235126>.
- [46] J.-M. Carter, V. V. Shankar, M. A. Zeb, and H.-Y. Kee, *Phys. Rev. B* **85**, 115105 (2012), URL <http://link.aps.org/doi/10.1103/PhysRevB.85.115105>.
- [47] M. Phillips and V. Aji, *Phys. Rev. B* **90**, 115111 (2014), URL <http://link.aps.org/doi/10.1103/PhysRevB.90.115111>.
- [48] Y. Chen, Y.-M. Lu, and H.-Y. Kee, *Nature communications* **6**, 6593 (2015).
- [49] M. Zeng, C. Fang, G. Chang, Y.-A. Chen, T. Hsieh, A. Bansil, H. Lin, and L. Fu, ArXiv e-prints (2015), 1504.03492.
- [50] C.-K. Chiu and A. P. Schnyder, *Phys. Rev. B* **90**, 205136 (2014), URL <http://link.aps.org/doi/10.1103/PhysRevB.90.205136>.
- [51] K. Mullen, B. Uchoa, and D. T. Glatzhofer, *Phys. Rev. Lett.* **115**, 026403 (2015), URL <http://link.aps.org/doi/10.1103/PhysRevLett.115.026403>.
- [52] H. Weng, Y. Liang, Q. Xu, R. Yu, Z. Fang, X. Dai, and Y. Kawazoe, *Phys. Rev. B* **92**, 045108 (2015), URL <http://link.aps.org/doi/10.1103/PhysRevB.92.045108>.
- [53] R. Yu, H. Weng, Z. Fang, X. Dai, and X. Hu, *Phys. Rev. Lett.* **115**, 036807 (2015), URL <http://link.aps.org/doi/10.1103/PhysRevLett.115.036807>.
- [54] Y. Kim, B. J. Wieder, C. L. Kane, and A. M. Rappe, *Phys. Rev. Lett.* **115**, 036806 (2015), URL

- <http://link.aps.org/doi/10.1103/PhysRevLett.115.036807>
- [55] G. Bian, T.-R. Chang, R. Sankar, S.-Y. Xu, H. Zheng, T. Neupert, C.-K. Chiu, S.-M. Huang, G. Chang, I. Belopolski, et al., *Nature Communications* **7**, 10556 (2016).
- [56] L. S. Xie, L. M. Schoop, E. M. Seibel, Q. D. Gibson, W. Xie, and R. J. Cava, *APL Mater.* **3**, 083602 (2015), URL <http://scitation.aip.org/content/aip/journal/aplmater/3/8/10.1063/1.4924545>, URL <http://link.aps.org/doi/10.1103/PhysRevX.4.031027>.
- [57] J.-W. Rhim and Y. B. Kim, *Phys. Rev. B* **92**, 045126 (2015), URL <http://link.aps.org/doi/10.1103/PhysRevB.92.045126>.
- [58] Y. Chen, Y. Xie, S. A. Yang, H. Pan, F. Zhang, M. L. Cohen, and S. Zhang, ArXiv e-prints (2015), 1505.02284.
- [59] C. Fang, Y. Chen, H.-Y. Kee, and L. Fu, *Phys. Rev. B* **92**, 081201 (2015), URL <http://link.aps.org/doi/10.1103/PhysRevB.92.081201>.
- [60] G. Bian, T.-R. Chang, H. Zheng, S. Velury, S.-Y. Xu, T. Neupert, C.-K. Chiu, S.-M. Huang, D. S. Sanchez, I. Belopolski, et al., *Phys. Rev. B* **93**, 121113 (2016), URL <http://link.aps.org/doi/10.1103/PhysRevB.93.121113>.
- [61] Y.-H. Chan, C.-K. Chiu, M. Y. Chou, and A. P. Schnyder, ArXiv e-prints (2015), 1510.02759.
- [62] N. H. Lindner, G. Refael, and V. Galitski, *Nature Physics* **7**, 490 (2011).
- [63] T. Kitagawa, T. Oka, A. Brataas, L. Fu, and E. Demler, *Phys. Rev. B* **84**, 235108 (2011), URL <http://link.aps.org/doi/10.1103/PhysRevB.84.235108>.
- [64] T. Oka and H. Aoki, *Phys. Rev. B* **79**, 081406 (2009), URL <http://link.aps.org/doi/10.1103/PhysRevB.79.081406>.
- [65] J.-i. Inoue and A. Tanaka, *Phys. Rev. Lett.* **105**, 017401 (2010), URL <http://link.aps.org/doi/10.1103/PhysRevLett.105.017401>.
- [66] Z. Gu, H. A. Fertig, D. P. Arovas, and A. Auerbach, *Phys. Rev. Lett.* **107**, 216601 (2011), URL <http://link.aps.org/doi/10.1103/PhysRevLett.107.216601>.
- [67] T. Kitagawa, M. S. Rudner, E. Berg, and E. Demler, *Phys. Rev. A* **82**, 033429 (2010), URL <http://link.aps.org/doi/10.1103/PhysRevA.82.033429>.
- [68] T. Kitagawa, E. Berg, M. Rudner, and E. Demler, *Phys. Rev. B* **82**, 235114 (2010), URL <http://link.aps.org/doi/10.1103/PhysRevB.82.235114>.
- [69] N. H. Lindner, D. L. Bergman, G. Refael, and V. Galitski, *Phys. Rev. B* **87**, 235131 (2013), URL <http://link.aps.org/doi/10.1103/PhysRevB.87.235131>.
- [70] L. Jiang, T. Kitagawa, J. Alicea, A. R. Akhmerov, D. Pekker, G. Refael, J. I. Cirac, E. Demler, M. D. Lukin, and P. Zoller, *Phys. Rev. Lett.* **106**, 220402 (2011), URL <http://link.aps.org/doi/10.1103/PhysRevLett.106.220402>.
- [71] M. S. Rudner, N. H. Lindner, E. Berg, and M. Levin, *Physical Review X* **3**, 031005 (2013).
- [72] J. P. Dahlhaus, J. M. Edge, J. Tworzydło, and C. W. J. Beenakker, *Phys. Rev. B* **84**, 115133 (2011), URL <http://link.aps.org/doi/10.1103/PhysRevB.84.115133>.
- [73] A. Gómez-León and G. Platero, *Phys. Rev. Lett.* **110**, 200403 (2013), URL <http://link.aps.org/doi/10.1103/PhysRevLett.110.200403>.
- [74] C.-K. Chan, P. A. Lee, K. S. Burch, J. H. Han, and Y. Ran, *Phys. Rev. Lett.* **116**, 026805 (2016), URL <http://link.aps.org/doi/10.1103/PhysRevLett.116.026805>.
- [75] L. M. Schoop, M. N. Ali, C. Straßer, V. Duppel, S. S. Parkin, B. V. Lotsch, and C. R. Ast, arXiv preprint arXiv:1509.00861 (2015).
- [76] J. Hu, Z. Tang, J. Liu, X. Liu, Y. Zhu, D. Graf, Y. Shi, S. Che, C. N. Lau, J. Wei, et al., arXiv preprint arXiv:1604.06860 (2016).
- [77] Y. Wu, L.-L. Wang, E. Mun, D. D. Johnson, D. Mou, L. Huang, Y. Lee, S. L. Budko, P. C. Canfield, and A. Kaminski, ArXiv e-prints (2016), 1603.00934.
- [78] J. L. Lu, W. Luo, X. Y. Li, S. Q. Yang, J. X. Cao, X. G. Gong, and H. J. Xiang, ArXiv e-prints (2016), 1603.04596.
- [79] N. Goldman and J. Dalibard, *Phys. Rev. Lett.* **110**, 106301 (2013), URL <http://link.aps.org/doi/10.1103/PhysRevLett.110.106301>.
- [80] A. G. Grushin, A. Gómez-León, and T. Neupert, *Phys. Rev. Lett.* **112**, 156801 (2014), URL <http://link.aps.org/doi/10.1103/PhysRevLett.112.156801>.
- [81] L. D'Alessio, ArXiv e-prints (2014), 1412.3481.
- [82] A. G. Grushin, Á. Gómez-León, and T. Neupert, ArXiv e-prints (2015), 1503.02580.
- [83] H. B. Nielsen and M. Ninomiya, *Nucl. Phys. B* **185**, 20 (1981).
- [84] R. Nair, P. Blake, A. Grigorenko, K. Novoselov, T. Booth, T. Stauber, N. Peres, and A. Geim, *Science* **320**, 1308 (2008).
- [85] Y. Wang, H. Steinberg, P. Jarillo-Herrero, and N. Gedik, *Science* **342**, 453 (2013).
- [86] G. Jotzu, M. Messer, R. Desbuquois, M. Lebrat, T. Uehlinger, D. Greif, and T. Esslinger, *Nature* **515**, 237 (2014).
- [87] C. V. Parker, L.-C. Ha, and C. Chin, *Nature Physics* **9**, 769 (2013).
- [88] W. Zheng and H. Zhai, *Phys. Rev. A* **89**, 061603 (2014), URL <http://link.aps.org/doi/10.1103/PhysRevA.89.061603>.
- [89] Y. T. Katan and D. Podolsky, *Phys. Rev. Lett.* **110**, 016802 (2013), URL <http://link.aps.org/doi/10.1103/PhysRevLett.110.016802>.
- [90] P. Hořava, *Phys. Rev. Lett.* **95**, 016405 (2005), URL <http://link.aps.org/doi/10.1103/PhysRevLett.95.016405>.
- [91] Y. X. Zhao and Z. D. Wang, *Phys. Rev. Lett.* **110**, 240404 (2013), URL <http://link.aps.org/doi/10.1103/PhysRevLett.110.240404>.
- [92] J. W. Milnor, *Morse theory*, 51 (Princeton university press, 1963).
- [93] For a simple narrative, we shall not distinguish between the terms “nodal line” and “nodal ring” hereafter.
- [94] In general, gapless band-touching is protected by the combination of topology and symmetry[90, 91].
- [95] In fancier words, this is a consequence of the Morse theory[92].

Supplemental Material

DEVIATION OF THE FORMULAS OF ANOMALOUS HALL CONDUCTIVITY

According to the linear response theory[64], the formula for the Hall conductivity is given by

$$\sigma_{\mu\nu} = e^2 \epsilon_{\mu\nu\rho} \int \frac{d^3k}{(2\pi)^3} \sum_{\alpha} f_{\alpha}(k) [\nabla_{\mathbf{k}} \times \mathcal{A}_{\alpha}(\mathbf{k})]_{\rho}, \quad (17)$$

where $\mathcal{A}_{\alpha}(\mathbf{k}) = -i \ll \Phi_{\alpha}(\mathbf{k}) | \nabla_{\mathbf{k}} | \Phi_{\alpha}(\mathbf{k}) \gg \equiv \frac{1}{T} \int_0^T dt \langle \Phi_{\alpha}(\mathbf{k}, t) | \nabla_{\mathbf{k}} | \Phi_{\alpha}(\mathbf{k}, t) \rangle$ with $T = 2\pi/\omega$ the driven period, and $\Phi_{\alpha}(\mathbf{k}, t)$ is the eigenvector of $[\mathcal{H}(\mathbf{k}, t) - i\partial_t] \Phi_{\alpha}(\mathbf{k}, t) = \epsilon_{\alpha}(k) \Phi_{\alpha}(\mathbf{k}, t)$ with $\Phi_{\alpha}(\mathbf{k}, t + T) = \Phi_{\alpha}(\mathbf{k}, t)$. Since $\Phi_{\alpha}(\mathbf{k}, t)$ is periodic, it can be expanded as $\Phi_{\alpha}(\mathbf{k}, t) = \sum_n e^{in\omega t} \Phi_{\alpha}^{(n)}(\mathbf{k})$ with $\Phi_{\alpha}^{(n)}(\mathbf{k})$ time-independent and satisfying the Floquet

equation

$$[\mathcal{E}_\alpha(k) - n\omega]\Phi_\alpha^{(n)}(\mathbf{k}) = \sum_m \mathcal{H}_{n-m}(\mathbf{k})\Phi_\alpha^{(m)}(\mathbf{k}) \quad (18)$$

with $\mathcal{H}_{n-m}(\mathbf{k}) = \frac{1}{T} \int_0^T dt e^{i(m-n)\omega t} \mathcal{H}(\mathbf{k}, t)$. Thus $\mathcal{A}_\alpha(\mathbf{k})$ can also be written as

$$\mathcal{A}_\alpha(\mathbf{k}) = \sum_n \mathcal{A}_{\alpha,n}(\mathbf{k}) = -i \sum_n \langle \Phi_\alpha^{(n)}(\mathbf{k}) | \nabla_{\mathbf{k}} | \Phi_\alpha^{(n)}(\mathbf{k}) \rangle \quad (19)$$

In the off-resonant regime (ω much larger than other energy scale), based on perturbation theory[63], it is found that

$$\begin{aligned} \mathcal{H}_{\text{eff}}(\mathbf{k})\Phi_\alpha^{(0)}(\mathbf{k}) &= E_\alpha(\mathbf{k})\Phi_\alpha^{(0)}(\mathbf{k}), \\ \Phi_\alpha^{(n)}(\mathbf{k}) &= -\frac{\mathcal{H}_n}{n\omega}\Phi_\alpha^{(0)}(\mathbf{k}) \quad \text{for } n \neq 0. \end{aligned} \quad (20)$$

where

$$\mathcal{H}_{\text{eff}}(\mathbf{k}) = \mathcal{H}_0 + \sum_{n \geq 1} \frac{[\mathcal{H}_{+n}, \mathcal{H}_{-n}]}{n\omega} + \mathcal{O}\left(\frac{1}{\omega^2}\right) \quad (21)$$

As has been obtained in the main text, $\mathcal{H}_{\text{eff}}(\mathbf{k})$ takes the following form,

$$\mathcal{H}_{\text{eff}}(\mathbf{k}) = [\tilde{m} - Bk^2]\tau_x + vk_z\tau_z + \lambda k_y\tau_y. \quad (22)$$

It is readily found that $E_{\alpha=\pm}(\mathbf{k}) = \pm \sqrt{[\tilde{m} - Bk^2]^2 + v^2k_z^2 + \lambda^2k_y^2}$, and $\Phi_\alpha^{(0)}(\mathbf{k})$ are given by

$$\Phi_+^{(0)}(\mathbf{k}) = \begin{pmatrix} \cos \frac{\theta_{\mathbf{k}}}{2} \\ \sin \frac{\theta_{\mathbf{k}}}{2} e^{i\varphi_{\mathbf{k}}} \end{pmatrix}, \Phi_-^{(0)}(\mathbf{k}) = \begin{pmatrix} \sin \frac{\theta_{\mathbf{k}}}{2} e^{-i\varphi_{\mathbf{k}}} \\ -\cos \frac{\theta_{\mathbf{k}}}{2} \end{pmatrix}, \quad (23)$$

where $\theta_{\mathbf{k}} = \arccos \frac{vk_z}{E_\pm(\mathbf{k})}$ and $\varphi_{\mathbf{k}} = \arctan \frac{\lambda k_y}{\tilde{m} - Bk^2}$. For the case that the occupation is close to equilibrium, namely, $f_{\pm,n}(k) = \delta_{n,0} n_\pm(E_\pm(\mathbf{k}))$, where $n_\pm(E_\pm(\mathbf{k})) = 1/(e^{(E_\pm(\mathbf{k}) - \mu)/T} + 1)$ is the Fermi-Dirac distribution. With the $\mathcal{O}(1/\omega^2)$ terms omitted, the Hall conductivity takes the following form:

$$\sigma_{\mu\nu} = e^2 \epsilon_{\mu\nu\rho} \int \frac{d^3k}{(2\pi)^3} \sum_{i=\pm} n_i(E_i(\mathbf{k})) [\nabla_{\mathbf{k}} \times \mathcal{A}_{i,0}(\mathbf{k})]_\rho. \quad (24)$$

A combination of Eq.(19) and Eq.(23) gives

$$\mathcal{A}_{+,0}(\mathbf{k}) = -\mathcal{A}_{-,0}(\mathbf{k}) = \sin^2 \frac{\theta_{\mathbf{k}}}{2} \nabla_{\mathbf{k}} \varphi_{\mathbf{k}}, \quad (25)$$

thus Eq.(24) can be rewritten as

$$\sigma_{\mu\nu} = \frac{e^2}{2} \epsilon_{\mu\nu\rho} \int \frac{d^3k}{(2\pi)^3} \sin \theta_{\mathbf{k}} [\nabla_{\mathbf{k}} \theta_{\mathbf{k}} \times \nabla_{\mathbf{k}} \varphi_{\mathbf{k}}]_\rho (n_+ - n_-), \quad (26)$$

this formula can be further rewritten as

$$\sigma_{\mu\nu} = \frac{e^2}{2} \int \frac{d^3k}{(2\pi)^3} [\hat{\mathbf{d}} \cdot (\partial_{k_\mu} \hat{\mathbf{d}} \times \partial_{k_\nu} \hat{\mathbf{d}})] (n_+ - n_-), \quad (27)$$

where $\hat{\mathbf{d}} = (\sin \theta_k \cos \varphi_{\mathbf{k}}, \sin \theta_k \sin \varphi_{\mathbf{k}}, \cos \theta_k)$. The unit vector $\hat{\mathbf{d}}$ can also be expressed in the form $\hat{\mathbf{d}} \equiv \mathbf{d}/|\mathbf{d}|$ with $\mathbf{d} = \text{Tr}[\tilde{\tau} \mathcal{H}_{\text{eff}}]/2$. A direct calculation leads to the final expression

$$\sigma_{yz} = \frac{e^2}{2} \int \frac{dk^3}{(2\pi)^3} \frac{\lambda v (\tilde{m} - 2Bk_x^2 + Bk^2)}{[E_+(k)]^3} (n_+ - n_-). \quad (28)$$

INCIDENT LIGHT IN THE z DIRECTION

In the main text we have focused on the cases that the incident light is in parallel with the plane of nodal line. Now we consider an incident light along the direction perpendicular to the plane of nodal line. Suppose that the system is coupled to an incident circularly polarized light in the z direction (perpendicular to the nodal-line plane), with the vector potential $\mathbf{A}(t) = A_0(\cos(\omega t), \sin(\omega t + \phi), 0)$, then the time-periodic Hamiltonian can be expanded as $\mathcal{H}(\mathbf{k}, t) = \sum_n \mathcal{H}_n(\mathbf{k}) e^{in\omega t}$, with the Fourier components

$$\begin{aligned} \mathcal{H}_0(\mathbf{k}) &= [m - Be^2 A_0^2 - Bk^2]\tau_x + vk_z\tau_z, \\ \mathcal{H}_{\pm 1}(\mathbf{k}) &= -eA_0 B(k_x \mp ie^{\pm i\phi} k_y)\tau_x, \\ \mathcal{H}_{\pm 2}(\mathbf{k}) &= -Be^2 A_0^2 (1 - e^{\pm i2\phi})\tau_x/4. \end{aligned} \quad (29)$$

and $\mathcal{H}_n = 0$ for $|n| > 2$. The effective Hamiltonian can be obtained as

$$\begin{aligned} \mathcal{H}_{\text{eff}}(\mathbf{k}) &= \mathcal{H}_0 + \sum_{n \geq 1} \frac{[\mathcal{H}_{+n}, \mathcal{H}_{-n}]}{n\omega} + \mathcal{O}\left(\frac{1}{\omega^2}\right) \\ &= [m - Be^2 A_0^2 - Bk^2]\tau_x + vk_z\tau_z, \end{aligned} \quad (30)$$

it is readily seen that the effect of the circularly polarized light perpendicular to the nodal-line plane is just to shrink of the nodal line, instead of producing Weyl points.